High-Resolution Photoelectron Imaging of Cryogenically-Cooled $C_{59}N^-$ and $(C_{59}N)_2^{2-}$ Azafullerene Anions

Guo-Zhu Zhu,[†] Yoshifumi Hashikawa,[‡] Yuan Liu,[†] Qian-Fan Zhang,[†] Ling Fung Cheung,[†] Yasujiro Murata,[‡] and Lai-Sheng Wang*,[†]

[†]Department of Chemistry, Brown University, Providence, Rhode Island 02912, United States
[‡]Institute for Chemical Research, Kyoto University, Uji, Kyoto 611-0011, Japan

S *Supporting Information*

ABSTRACT: We report a photoelectron imaging study of cryogenically cooled $C_{59}N^-$ and $(C_{59}N)_2^{2-}$ anions produced from electrospray ionization. High-resolution photoelectron spectra are obtained for $C_{59}N^-$ for the first time, allowing seven vibrational frequencies of the $C_{59}N$ azafullerene to be measured. The electron affinity of $C_{59}N$ is determined accurately to be 3.0150 ± 0.0007 eV. The observed vibrational features are understood on the basis of calculated frequencies and compared with those of C_{60} and $C_{59}HN$. The photoelectron image of $(C_{59}N)_2^{2-}$, which has the same mass/charge ratio as $C_{59}N^-$, is also observed, allowing the second electron affinity of the $(C_{59}N)_2$ azafullerene dimer to be measured as 1.20 ± 0.05 eV. The intramolecular Coulomb repulsion of the $(C_{59}N)_2^{2-}$ dianion is estimated to be 1.96 eV and is investigated theoretically using the electron density difference between $(C_{59}N)_2^{2-}$ and $(C_{59}N)_2$.
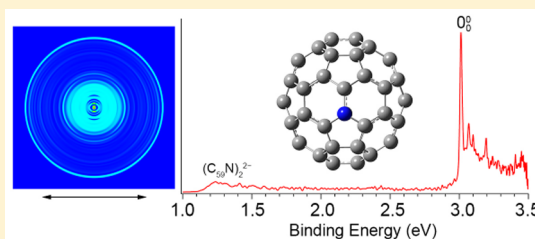
Azafullerene ($C_{59}N$), with one carbon atom in C_{60} substituted by a nitrogen atom, has received particular attention due to its unique electronic and chemical properties.[1,2] The N-substitution results in an *n*-type doping, adding one electron to the close-shell π system of C_{60}.[3,4] The extra unpaired electron is mainly localized on the C atom that is closest to the N atom in the [6,6] closed structure and exhibits sp^3 character.[5-10] Hence, $C_{59}N$ is a reactive radical and can easily dimerize.[1,2,7-10] The $C_{59}N^+$ cation is isoelectronic to C_{60} and was first observed as a gaseous species.[11] The first macroscopic synthesis of $C_{59}N$ was in its dimer form, $(C_{59}N)_2$,[12] allowing its physical and chemical properties to be characterized by a variety of techniques.[13-27] Most interestingly, the azafullerene has promising applications in molecular electronics as the basis for single-molecule rectifiers,[28-30] field-effect transistors,[31,32] and electron donor−acceptor systems.[33-35] However, the electron affinity (EA) of $C_{59}N$, one of its most fundamental electronic and thermodynamic properties, is still not known experimentally. Theoretical calculations suggested an EA for $C_{59}N$ to be around 2.70 eV,[5,7] which is comparable to the EA of C_{60} accurately known to be 2.6835 eV.[36] In a C_{60}-$C_{59}N$ dyad,[33] a higher reduction potential was observed for $C_{59}N$ than C_{60}, indicating a higher EA for $C_{59}N$ than C_{60}.

In the current study, we present a high-resolution photoelectron imaging (PEI) study of cryogenically cooled $C_{59}N^-$ anions produced from an electrospray ionization source. Vibrationally resolved photoelectron spectra at various photon energies have been obtained, allowing us to measure the EA of $C_{59}N$ accurately for the first time to be 3.0150 eV, which is 0.3315 eV higher than that of C_{60}. Seven vibrational frequencies

are also obtained for $C_{59}N$, five of which are found to be similar to those observed in the high-resolution photoelectron spectra of C_{60}^-.[36] Additionally, we have also obtained the photoelectron spectrum for the parent $(C_{59}N)_2^{2-}$ dimer dianion, which has the same mass/charge ratio as $C_{59}N^-$, yielding the second EA of $(C_{59}N)_2$ to be 1.20 eV. The intramolecular Coulomb repulsion in the dimer dianion is estimated to be 1.96 eV. The extra charges in the dianion are shown to be more localized at the two ends of the dimer due to the electron−electron repulsion.

The experiment was carried out using our third-generation electrospray PEI apparatus,[37] equipped with a cryogenically cooled Paul trap[38] and a high-resolution PEI system.[39] A sample of azafullerene dimer, $(C_{59}N)_2$,[12,40] was dissolved in a mixed solvent of *ortho*-dichlorobenzene/CH_3CN (1/3 ratio in volume), to which a reducing agent, tetrakis(dimethylamino)-ethylene (TDAE) prepared from tris(dimethylamino)-methane,[41,42] was added. The resulting solution was electrosprayed, and anions from the source were guided into a cryogenically controlled Paul trap operated at 4.5 K and thermally cooled via collisions with 1 mTorr He/H_2 (4/1 in volume) background gas.[38] The cold anions were pulsed out at a 10 Hz repetition rate into the extraction zone of a time-of-flight mass spectrometer. The main anion signal observed was at *m/z* = 722, which could be due to either $C_{59}N^-$ or $(C_{59}N)_2^{2-}$, because our time-of-flight mass spectrometer did not have high enough resolution to resolve the isotopic

distribution. Since the $(C_{59}N)_2$ dimer has a relatively small dissociation energy,[23] it was expected to easily cleave upon reduction to $C_{59}N^-$ either in the solution or during the electrospray. The anions with $m/z = 722$ were selected by a mass gate and photodetached by the third harmonic of a Nd:YAG laser (354.7 nm) and a tunable dye laser in the interaction zone of the PEI system.[39] The photoelectron images were inverse-Abel transformed and reconstructed using both pBasex and BASEX.[43,44] The photoelectron spectra were calibrated with the known spectra of Au^- at different photon energies. The kinetic energy (KE) resolution was 3.8 cm^{-1} for electrons with 55 cm^{-1} KE and about 1.5% ($\Delta KE/KE$) for KE above 1 eV in the current experiment.

Figure 1 displays the PE image and spectrum of the anion at $m/z = 722$ at a photon energy of 354.7 nm. The spectrum
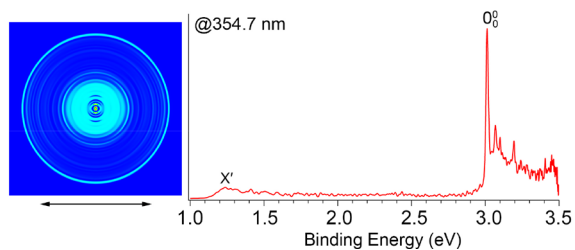

Figure 1. Photoelectron image and spectrum of $C_{59}N^-$ and $(C_{59}N)_2^{2-}$ at 354.7 nm. The weak peak labeled X′ represents detachment from $(C_{59}N)_2^{2-}$, while peak 0_0^0 denotes the detachment threshold of $C_{59}N^-$. The double arrow below the image indicates the directions of the laser polarization. Note the image corresponding to peak X′ is cut off.

reveals two detachment regions: a weak and broad peak (X′) at around 1.2 eV and a group of more intense peaks above 3 eV. This spectral pattern immediately suggested that the $m/z = 722$ mass signals contained both $C_{59}N^-$ and $(C_{59}N)_2^{2-}$. The 1.2 eV peak should come from the dianion, which is expected to have low binding energies due to the strong intramolecular Coulomb repulsion.[45] This low binding energy is comparable to that for a

similar dianion, $[C_{60}OC_{60}]^{2-}$, which has an electron binding energy of 1.02 eV.[46] The strong peaks above 3.0 eV, which display some resemblance to the 354.7 nm spectrum of C_{60}^-,[36] should come from $C_{59}N^-$, representing transitions from the ground vibrational level of the anion to vibrational levels of the electronic ground state of neutral $C_{59}N$. The first intense peak labeled 0_0^0 defines the EA of $C_{59}N$, which is more accurately measured to be 3.0150 ± 0.0007 eV in Figure 2a to be discussed below. It should be noted that, because of the existence of the repulsive Coulomb barrier, no low-energy electrons are allowed for detachment from the $(C_{59}N)_2^{2-}$ dianion,[45] i.e., the spectral region for $C_{59}N^-$ above 3 eV should contain no contributions from higher binding energy detachment transitions from the dianion.

To better resolve the vibrational peaks for $C_{59}N$, we took high-resolution photoelectron images at six different wavelengths near the detachment threshold, as shown in Figure 2. PEI allows low-energy electrons to be detected, significantly improving the spectral resolution for near-threshold detachment transitions.[39,47] At 409.80 nm in Figure 2a, peak 0_0^0 corresponds to an electron kinetic energy of 84 cm^{-1} and a line width (fwhm) of 12 cm^{-1}, yielding the most accurate value for the EA of $C_{59}N$ as 3.0150 ± 0.0007 eV. As reported previously,[48−50] anions in our cryogenic Paul trap have a rotational temperature of ∼30 K. Thus, the near-threshold peak width should mainly come from rotational broadening. Because of the p-wave detachment character, the cross section for the near-threshold detachment was quite low, as can be seen from the relatively poor signal/noise ratios in Figure 2a. The EA of $C_{59}N$ is 0.3315 eV higher than that of C_{60} at 2.6835 eV.[36]

By tuning the photon energies above the threshold systematically, we were able to resolve seven additional vibrational peaks, labeled from A to G, up to a binding energy of 3.15 eV, as shown in Figure 2b−f. The observed peaks, their binding energies, and the shifts from peak 0_0^0 (i.e., the measured fundamental vibrational frequencies of $C_{59}N$) are summarized in Table 1 and compared with our computed
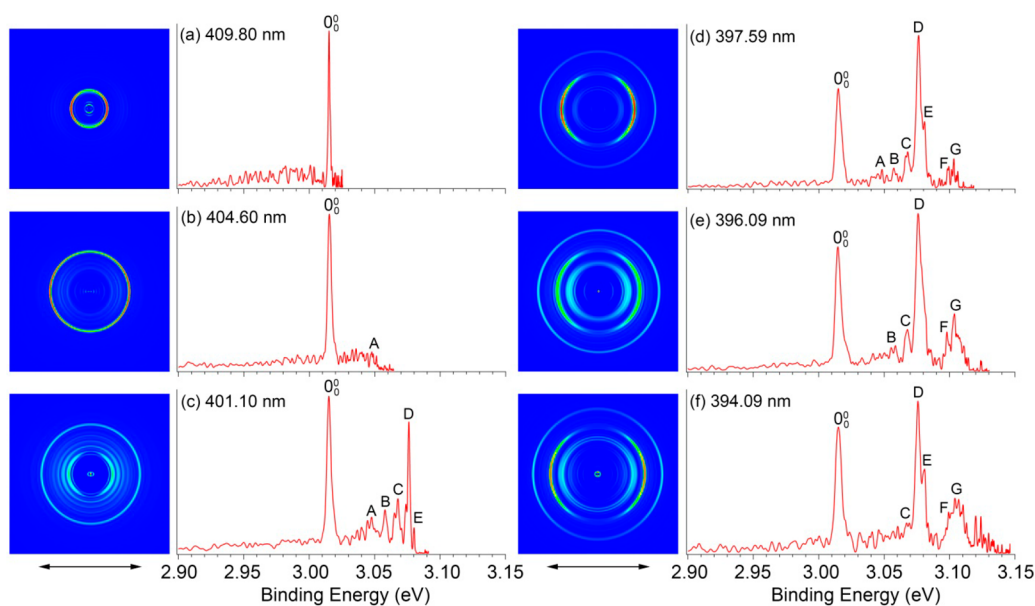

Figure 2. Photoelectron images and spectra of $C_{59}N^-$ at six different wavelengths. The double arrow below the images indicates the directions of the laser polarization.

frequencies for $C_{59}N$ (see Table S1 for all the 174 calculated frequencies), as well as those of C_{60} and $C_{59}HN$.

Table 1. Observed Vibrational Peaks, Their Binding Energies (BE) from the Photoelectron Spectra of $C_{59}N^{-}$ [a]

peak	BE (eV)	shift (cm⁻¹)	vibrational frequencies (cm⁻¹)			
			C_{60}^{-} [b]	solid C_{60} [c]	$C_{59}HN$ [d]	theo. $C_{59}N$ [e]
0_0^0	3.0150(7)	0				
A	3.0473(12)	260	262	262, $H_g(1)$	261.5	ν_1 (258)
				268, $H_g(1)$	271	ν_2 (262)
						ν_3 (268)
B	3.0573(10)	341	348	340, $T_{2u}(1)$		ν_4 (337)
				353, $G_u(1)$		ν_5 (342)
						ν_6 (350)
C	3.0673(10)	421		431, $H_g(2)$	424	ν_{10} (418)
					427	
D	3.0760(7)	492		494, $A_g(1)$	492	ν_{15} (498)
E	3.0805(10)	528	531	526, $T_{1u}(1)$	523	ν_{17} (524)
				534, $H_u(2)$	529	ν_{18} (532)
					531	ν_{19} (535)
F	3.0986(7)	674	670	668, $H_u(3)$		ν_{26} (675)
						ν_{27} (678)
G	3.1035(7)	713	717	709, $H_g(3)$		ν_{30} (718)
				713, $T_{2u}(2)$		ν_{31} (720)

[a]Their relative shifts to peak 0_0^0 are compared with the vibrational frequencies of C_{60} and $C_{59}HN$, as well as our calculated frequencies for $C_{59}N$. [b]Reference 36: 16 vibrational frequencies of C_{60} were measured by high-resolution PE imaging of cold C_{60}^{-}. [c]Reference 51: Vibrational frequencies of C_{60} were measured by inelastic neutron scattering of solid C_{60}. [d]Reference 52: Vibrational frequencies of $C_{59}HN$ were measured by IR and Raman spectroscopy. [e]The vibrational frequencies of $C_{59}N$ calculated at the B3LYP/Def2SVP level (see Table S1).

Because of the structural similarities between $C_{59}N$ and C_{60} or $C_{59}HN$, we expect that they should share similar vibrational properties. Indeed, peaks A, B, and E−G, with shifts of 260, 341, 528, 674, and 713 cm⁻¹, are in good agreement with the vibrational frequencies of C_{60} obtained from our previous PEI study of the cold C_{60}^{-} anion,[36] as well as those from inelastic neutron scattering of solid C_{60}.[51] The significant vibrational activities observed in the high-resolution PEI of cold C_{60}^{-} were due to the Jahn−Teller effect in C_{60}^{-} ($^2T_{1u}$), which does not have the I_h symmetry of neutral C_{60}. On the other hand, the substitution of a C by a N atom in C_{60} lowers the symmetry of $C_{59}N$ to C_s.[8] Since neutral $C_{59}N$ ($^2A'$) and $C_{59}N^{-}$ ($^1A'$) both have C_s symmetry, all vibrational modes with A' symmetry are allowed in the photodetachment. We computed the vibrational frequencies of neutral $C_{59}N$ at the B3LYP/Def2SVP level[53] and found 89 A' and 85 A'' modes, as given in Table S1. Because there is no vibrational degeneracy for the C_s $C_{59}N$, many vibrational modes have close frequencies, making unique assignments of the observed vibrational features for $C_{59}N$ challenging.

Comparing the experimental frequencies with the computed frequencies, we found that peaks A, B, and E can each be assigned to three possible A' modes with close frequencies, while peaks F and G can each be assigned to two possible A' modes, as shown in Table 1. Only peaks C and D, with shifts of 421 and 492 cm⁻¹, can be possibly assigned uniquely to

vibrational mode ν_{10} (418 cm⁻¹) and mode ν_{15} (498 cm⁻¹), respectively. The ν_{10} mode involves strong stretching of the N atom, while the ν_{15} mode is a totally symmetric breathing mode, as shown in Figure S1. Note that peak D is the most intense vibrational feature in Figure 2d−f. Similarly, one vibrational peak with frequency of 531 cm⁻¹ in the photoelectron spectra of C_{60}^{-} was observed to be dominant at lower photon energies. This non-Franck−Condon and photon-energy-dependent vibrational intensities were interpreted previously as being due to a strong Hertzberg−Teller coupling in C_{60}^{-}.[36] The dominant intensity of peak D in Figure 2 may be due to similar vibronic coupling effects in $C_{59}N^{-}$. The vibrational frequencies of $C_{59}HN$ have been measured by IR and Raman spectroscopy in the form of thin solid films.[52] A number of the vibrational frequencies of $C_{59}N$ obtained in the current study are similar to those measured for $C_{59}HN$, as shown in Table 1.

The photoelectron images in Figure 2 all exhibit distinct p-wave character with the photoelectron angular distributions parallel to the direction of the laser polarization, indicating that photodetachment of $C_{59}N^{-}$ is from a s-type orbital. This observation is consistent with the partial localization of the HOMO on the N atom and the nearby C atom, which shows sp^3 character (Figure S2).[5−10]

Even though the closed-shell $(C_{59}N)_2$ dimer was the parent azafullerene used to prepare the ESI solution, and it was known to be stable in solution,[1,2] the weak intensity of peak X′ compared to peak 0_0^0 in Figure 1 suggested that the majority of the $(C_{59}N)_2$ dimer was dissociated to the monomer either during the reduction by TDAE or in the ESI source. Assuming that $(C_{59}N)_2^{2-}$ and $C_{59}N^{-}$ have similar detachment cross sections at 354.7 nm, we estimated that the $(C_{59}N)_2^{2-}$ intensity was only ∼5% of that for $C_{59}N^{-}$ in the m/z = 722 mass peak. The low binding energy peak X′ in Figure 1 represents the detachment transition from $(C_{59}N)_2^{2-}$ to $(C_{59}N)_2^{-}$, yielding the second EA of $(C_{59}N)_2$ to be 1.20(5) eV. The first EA of $(C_{59}N)_2$ was calculated to be 2.85 eV, 0.15 eV higher than the calculated EA of $C_{59}N$ (2.70 eV).[7] If we assume the same error in the calculated EAs for the monomer and the dimer, we estimated the first EA of $(C_{59}N)_2$ to be ∼3.16 eV. The difference between the first and second EA of $(C_{59}N)_2$ can be viewed as the intramolecular Coulomb repulsion between the two extra charges in $(C_{59}N)_2^{2-}$, which is estimated as 1.96 eV. In fact, the difference between the electron binding energies of $C_{59}N^{-}$ and $(C_{59}N)_2^{2-}$ (1.82 eV) gives a similar intramolecular Coulomb repulsion. The intramolecular electron−electron repulsion in the fullerene dianions, C_n^{2-} (n = 70, 76, 78, 84) were estimated to be in the range of 2.745−2.37 eV, with smaller values for the larger fullerenes.[54,55] The even smaller value of 1.96 eV in $(C_{59}N)_2^{2-}$ is consistent with its larger molecular size. The C−C bond between the two $C_{59}N$ units in the azafullerene dimer is known to be quite weak, estimated to be only 7 kcal/mol (0.3 eV) by a thermal homolysis study.[23] The Coulomb repulsion between the two extra charges in the dianion is much larger than the C−C bond energy, indicating that the $(C_{59}N)_2^{2-}$ dianion is metastable relative to the bond cleavage to form two $C_{59}N^{-}$ monoanions. This result is consistent with the weak intensity of the dianion in the mass spectrum.

To further understand the intramolecular Coulomb repulsion in $(C_{59}N)_2^{2-}$, we calculated the difference of the total electron density ($\Delta\rho$) between $(C_{59}N)_2^{2-}$ and $(C_{59}N)_2$ at the B3LYP/6-311++G(d,p) level,[53] as shown in Figure 3a. We used the

(a) $\rho[(C_{59}N)_2{}^{2-} - (C_{59}N)_2]$

(b) $\rho[C_{59}N^- - C_{59}N]$
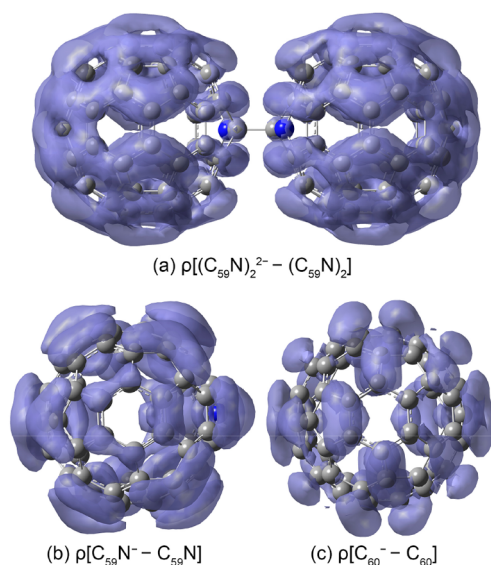
(c) $\rho[C_{60}{}^- - C_{60}]$

Figure 3. Differences of the total electron density ($\Delta\rho$) between: (a) $(C_{59}N)_2{}^{2-}$ and $(C_{59}N)_2$, (b) $C_{59}N^-$ and $C_{59}N$, and (c) $C_{60}{}^-$ and C_{60}. The calculations were done at the level of B3LYP/6-311++G(d,p).

optimized geometries under the same level of theory and basis sets for both the dianion and neutral. For comparison, we also computed the $\Delta\rho$ between $C_{59}N^-$ and $C_{59}N$ (Figure 3b), as well as that between $C_{60}{}^-$ and C_{60} (Figure 3c). As shown in Figure 3a, the extra electrons are delocalized over the surface of the azafullerene dimer with less density near the N atoms but higher density on the two ends. The uneven charge distribution is consistent with the expected Coulomb repulsion between the two extra electrons, and it is quite different from the localization of the HOMO on the N atoms in neutral $(C_{59}N)_2$.[5-7,13,14] In comparison, the extra electron in $C_{59}N^-$ is delocalized over the azafullerene surface with slightly more charge localized on the N atom (Figure 3b), while the extra charge in $C_{60}{}^-$ is evenly distributed over the fullerene surface (Figure 3c).

In conclusion, we report the first high-resolution photoelectron imaging study of $C_{59}N^-$ and the first observation of the azafullerene dimer dianion $(C_{59}N)_2{}^{2-}$. The EA of $C_{59}N$ is measured accurately to be 3.0150(7) eV. Seven vibrational frequencies are also obtained for $C_{59}N$ and are assigned by comparing with calculated frequencies and those of C_{60} and $C_{59}HN$. Similar vibrational frequencies are observed for the three species, suggesting relatively small geometry changes upon substitution of one C by one N atom on the C_{60} cage. The photoelectron spectrum of the $(C_{59}N)_2{}^{2-}$ dimer dianion yielded a second EA for $(C_{59}N)_2$ to be 1.20(5) eV. The intramolecular Coulomb repulsion between the two extra charges in the dimer dianion was estimated to be 1.96 eV, much higher than the C–C bond linking the dimer, suggesting that $(C_{59}N)_2{}^{2-}$ is metastable relative to dissociation to two $C_{59}N^-$; i.e., the $(C_{59}N)_2{}^{2-} \rightarrow 2C_{59}N^-$ reaction is exothermic. The intramolecular electron repulsion is investigated by the difference of the total electron density between $(C_{59}N)_2{}^{2-}$ and $(C_{59}N)_2$, revealing that the extra charges are pushed away from each other toward the two ends of the azafullerene dimer.

■ **AUTHOR INFORMATION**

Corresponding Author

*E-mail: Lai-Sheng_Wang@brown.edu.

ORCID ⓘ

Yoshifumi Hashikawa: 0000-0001-7834-9593

Yasujiro Murata: 0000-0003-0287-0299

Lai-Sheng Wang: 0000-0003-1816-5738

Notes

The authors declare no competing financial interest.

■ **REFERENCES**

(1) Hirsch, A.; Nuber, B. Nitrogen Heterofullerenes. *Acc. Chem. Res.* **1999**, *32*, 795−804.

(2) Vostrowsky, O.; Hirsch, A. Heterofullerenes. *Chem. Rev.* **2006**, *106*, 5191−5207.

(3) Andreoni, W.; Gygi, F.; Parrinello, M. Impurity States in Doped Fullerenes: $C_{59}B$ and $C_{59}N$. *Chem. Phys. Lett.* **1992**, *190*, 159−162.

(4) Kaneko, T.; Li, Y.; Nishigaki, S.; Hatakeyama, R. Azafullerene Encapsulated Single-Walled Carbon Nanotubes with *n*-Type Electrical Transport Property. *J. Am. Chem. Soc.* **2008**, *130*, 2714−2715.

(5) Andreoni, W.; Curioni, A.; Holczer, K.; Prassides, K.; Keshavarz-K, M.; Hummelen, J. C.; Wudl, F. Unconventional Bonding of Azafullerenes: Theory and Experiment. *J. Am. Chem. Soc.* **1996**, *118*, 11335−11336.

(6) Pichler, T.; Knupfer, M.; Golden, M. S.; Haffner, S.; Friedlein, R.; Fink, J.; Andreoni, W.; Curioni, A.; Keshavarz-K, M.; Bellavia-Lund, C.; et al. On-Ball Doping of Fullerenes: The Electronic Structure of $C_{59}N$ Dimers from Experiment and Theory. *Phys. Rev. Lett.* **1997**, *78*, 4249−4252.

(7) Andreoni, W. Computational Approach to the Physical Chemistry of Fullerenes and Their Derivatives. *Annu. Rev. Phys. Chem.* **1998**, *49*, 405−439.

(8) Ren, A.; Feng, J.; Sun, X.; Li, W.; Tian, W.; Sun, C.; Zheng, X.; Zerner, M. C. Theoretical Investigation of the Heterofullerenes $C_{59}N$ and $C_{69}N$ and Their Dimers. *Int. J. Quantum Chem.* **2000**, *78*, 422−436.

(9) Erbahar, D.; Susi, T.; Rocquefelte, X.; Bittencourt, C.; Scardamaglia, M.; Blaha, P.; Guttmann, P.; Rotas, G.; Tagmatarchis, N.; Zhu, X.; et al. Spectromicroscopy of C_{60} and Azafullerene $C_{59}N$: Identifying Surface Adsorbed Water. *Sci. Rep.* **2016**, *6*, 35605.

(10) Bellavia-Lund, C.; Keshavarz-K, M.; Collins, T.; Wudl, F. Fullerene Carbon Resonance Assignments through $^{15}N-^{13}C$ Coupling Constants and Location of the sp^3 Carbon Atoms of $(C_{59}N)_2$. *J. Am. Chem. Soc.* **1997**, *119*, 8101−8102.

(11) Lamparth, I.; Nuber, B.; Schick, G.; Skiebe, A.; Grosser, T.; Hirsch, A. $C_{59}N^+$ and $C_{69}N^+$: Isoelectronic Heteroanalogues of C_{60} and C_{70}. *Angew. Chem., Int. Ed. Engl.* **1995**, *34*, 2257−2259.

(12) Hummelen, J. C.; Knight, B.; Pavlovich, J.; Gonzalez, R.; Wudl, F. Isolation of the Heterofullerene $C_{59}N$ as Its Dimer $(C_{59}N)_2$. *Science* **1995**, *269*, 1554−1556.

(13) Haffner, S.; Pichler, T.; Knupfer, M.; Umlauf, B.; Friedlein, R.; Golden, M. S.; Fink, J.; Keshavarz-K, M.; Bellavia-Lund, C.; Sastre, A.; et al. The Electronic Structure of $(C_{59}N)_2$ from High Energy Spectroscopy. *Eur. Phys. J. B* **1998**, *1*, 11−17.

(14) Hunt, M. R. C.; Pichler, T.; Siller, L.; Bruhwiler, P. A.; Golden, M. S.; Tagmatarchis, N.; Prassides, K.; Rudolf, P. Final-State

Interference Effects in Valence Band Photoemission of $(C_{59}N)_2$. *Phys. Rev. B: Condens. Matter Mater. Phys.* **2002**, *66*, 193404.

(15) Schulte, K.; Wang, L.; Moriarty, P. J.; Prassides, K.; Tagmatarchis, N. Resonant Processes and Coulomb Interactions in $(C_{59}N)_2$. *J. Chem. Phys.* **2007**, *126*, 184707.

(16) Deng, Y.; Gao, B.; Deng, M.; Luo, Y. A Comparative Theoretical Study on Core-Hole Excitation Spectra of Azafullerene and Its Derivatives. *J. Chem. Phys.* **2014**, *140*, 124304.

(17) Kuzmany, H.; Plank, W.; Winter, J.; Dubay, O.; Tagmatarchis, N.; Prassides, K. Raman Spectrum and Stability of $(C_{59}N)_2$. *Phys. Rev. B: Condens. Matter Mater. Phys.* **1999**, *60*, 1005−1012.

(18) Plank, W.; Pichler, T.; Kuzmany, H.; Dubay, O.; Tagmatarchis, N.; Prassides, K. Resonance Raman Excitation and Electronic Structure of the Single Bonded Dimers $(C_{60}^-)_2$ and $(C_{59}N)_2$. *Eur. Phys. J. B* **2000**, *17*, 33−42.

(19) Krause, M.; Baes-Fischlmair, S.; Pfeiffer, R.; Plank, W.; Pichler, T.; Kuzmany, H.; Tagmatarchis, N.; Prassides, K. Thermal Stability and High Temperature Graphitization of Bisazafullerene $(C_{59}N)_2$ as Studied by IR and Raman Spectroscopy. *J. Phys. Chem. B* **2001**, *105*, 11964−11969.

(20) Auerhammer, J. M.; Kim, T.; Knupfer, M.; Golden, M. S.; Fink, J.; Tagmatarchis, N.; Prassides, K. Vibrational and Electronic Excitations of $(C_{59}N)_2$. *Solid State Commun.* **2001**, *117*, 697−701.

(21) Gruss, A.; Dinse, K. P.; Hirsch, A.; Nuber, B.; Reuther, U. Photolysis of $(C_{59}N)_2$ Studied by Time-Resolved EPR. *J. Am. Chem. Soc.* **1997**, *119*, 8728−8729.

(22) Hasharoni, K.; Bellavia-Lund, C.; Keshavarz-K, M.; Srdanov, G.; Wudl, F. Light-Induced ESR Studies of the Heterofullerene Dimers. *J. Am. Chem. Soc.* **1997**, *119*, 11128−11129.

(23) Simon, F.; Arcon, D.; Tagmatarchis, N.; Garaj, S.; Forro, L.; Prassides, K. ESR Signal in Azafullerene $(C_{59}N)_2$ Induced by Thermal Homolysis. *J. Phys. Chem. A* **1999**, *103*, 6969−6971.

(24) Butcher, M. J.; Jones, F. H.; Beton, P. H.; Moriarty, P.; Cotier, B. N.; Upward, M. D.; Prassides, K.; Kordatos, K.; Tagmatarchis, N.; Wudl, F.; et al. $C_{59}N$ Monomers: Stabilization Through Immobilization. *Phys. Rev. Lett.* **1999**, *83*, 3478−3481.

(25) Butcher, M. J.; Jones, F. H.; Moriarty, P.; Beton, P. H.; Prassides, K.; Kordatos, K.; Tagmatarchis, N. Room Temperature Manipulation of the Heterofullerene $C_{59}N$ on Si(100)-2 × 1. *Appl. Phys. Lett.* **1999**, *75*, 1074−1076.

(26) Jones, F. H.; Butcher, M. J.; Cotier, B. N.; Moriarty, P.; Beton, P. H.; Dhanak, V. R.; Prassides, K.; Kordatos, K.; Tagmatarchis, N.; Wudl, F. Oscillations in the Valence-Band Photoemission Spectrum of the Heterofullerene $C_{59}N$: A Photoelectron Interference Phenomenon. *Phys. Rev. B: Condens. Matter Mater. Phys.* **1999**, *59*, 9834−9837.

(27) Silien, C.; Marenne, I.; Auerhammer, J.; Tagmatarchis, N.; Prassides, K.; Thiry, P. A.; Rudolf, P. Adsorption of Fullerene and Azafullerene on Cu(111) Studied by Electron Energy Loss Spectroscopy. *Surf. Sci.* **2001**, *482−485*, 1−8.

(28) Zhao, J.; Zeng, C.; Cheng, X.; Wang, K.; Wang, G.; Yang, J.; Hou, J. G.; Zhu, Q. Single $C_{59}N$ Molecule as a Molecular Rectifier. *Phys. Rev. Lett.* **2005**, *95*, 045502.

(29) Fang, C.; Zhao, P.; Cui, B.; Wang, L.; Liu, D.; Xie, S. Current Rectification in Single Molecule $C_{59}N$: Effect of Molecular Polarity Induced Dipole Moment. *Phys. Lett. A* **2010**, *374*, 4465−4470.

(30) Tawfik, S. A.; Cui, X. Y.; Ringer, S. P.; Stampfl, C. Electrical Rectification of $C_{59}N$: The Role of Anchoring and Doping Sites. *J. Chem. Phys.* **2016**, *144*, 021101.

(31) Kumashiro, R.; Tanigaki, K.; Ohashi, H.; Tagmatarchis, N.; Kato, H.; Shinohara, H.; Akasaka, T.; Kato, K.; Aoyagi, S.; Kimura, S.; et al. Azafullerene $(C_{59}N)_2$ Thin-Film Field-Effect Transistors. *Appl. Phys. Lett.* **2004**, *84*, 2154−2156.

(32) Li, Y.; Kaneko, T.; Kong, J.; Hatakeyama, R. Photoswitching in Azafullerene Encapsulated Single-Walled Carbon Nanotube FET Devices. *J. Am. Chem. Soc.* **2009**, *131*, 3412−3413.

(33) Hauke, F.; Herranz, M. A.; Echegoyen, L.; Guldi, D.; Hirsch, A.; Atalick, S. The First Fullerene-Heterofullerene Dyad. *Chem. Commun.* **2004**, 600−601.

(34) Rotas, G.; Tagmatarchis, N. Azafullerene $C_{59}N$ in Donor−Acceptor Dyads: Synthetic Approaches and Properties. *Chem. - Eur. J.* **2016**, *22*, 1206−1214.

(35) Rotas, G.; Martín-Gomis, L.; Ohkubo, K.; Fernandez-Lazaro, F.; Fukuzumi, S.; Tagmatarchis, N.; Sastre-Santos, A. Axially Substituted Silicon Phthalocyanine as Electron Donor in a Dyad and Triad with Azafullerene as Electron Acceptor for Photoinduced Charge Separation. *Chem. - Eur. J.* **2016**, *22*, 15137−15143.

(36) Huang, D. L.; Dau, P. D.; Liu, H. T.; Wang, L. S. High-Resolution Photoelectron Imaging of Cold C_{60}^- Anions and Accurate Determination of the Electron Affinity of C_{60}. *J. Chem. Phys.* **2014**, *140*, 224315.

(37) Wang, L. S. Electrospray Photoelectron Spectroscopy: From Multiply-Charged Anions to Ultracold Anions. *J. Chem. Phys.* **2015**, *143*, 040901.

(38) Wang, X. B.; Wang, L. S. Development of a Low-Temperature Photoelectron Spectroscopy Instrument Using an Electrospray Ion Source and a Cryogenically Controlled Ion Trap. *Rev. Sci. Instrum.* **2008**, *79*, 073108.

(39) León, I.; Yang, Z.; Liu, H. T.; Wang, L. S. The Design and Construction of a High-Resolution Velocity-Map Imaging Apparatus for Photoelectron Spectroscopy Studies of Size-Selected Clusters. *Rev. Sci. Instrum.* **2014**, *85*, 083106.

(40) Hashikawa, Y.; Murata, M.; Wakamiya, A.; Murata, Y. Synthesis and Properties of Endohedral Aza[60]fullerenes: $H_2O@C_{59}N$ and $H_2@C_{59}N$ as Their Dimers and Monomers. *J. Am. Chem. Soc.* **2016**, *138*, 4096−4104.

(41) Broggi, J.; Terme, T.; Vanelle, P. Organic Electron Donors as Powerful Single-Electron Reducing Agents in Organic Synthesis. *Angew. Chem., Int. Ed.* **2014**, *53*, 384−413.

(42) Mahesh, M.; Murphy, J. A.; LeStrat, F.; Wessel, H. P. Reduction of Arenediazonium Salts by Tetrakis(dimethylamino)ethylene (TDAE): Efficient Formation of Products Derived from Aryl Radicals. *Beilstein J. Org. Chem.* **2009**, *5*, 1−12.

(43) Garcia, G. A.; Nahon, L.; Powis, I. Two-Dimensional Charged Particle Image Inversion Using a Polar Basis Function Expansion. *Rev. Sci. Instrum.* **2004**, *75*, 4989.

(44) Dribinski, V.; Ossadtchi, A.; Mandelshtam, V. A.; Reisler, H. Reconstruction of Abel-Transformable Images: The Gaussian Basis-Set Expansion Abel Transform Method. *Rev. Sci. Instrum.* **2002**, *73*, 2634.

(45) Wang, L. S.; Wang, X. B. Probing Free Multiply Charged Anions Using Photodetachment Photoelectron Spectroscopy. *J. Phys. Chem. A* **2000**, *104*, 1978−1990.

(46) Wang, X. B.; Matheis, K.; Ioffe, I. N.; Goryunkov, A. A.; Yang, J.; Kappes, M. M.; Wang, L. S. High Resolution and Low-Temperature Photoelectron Spectroscopy of an Oxygen-Linked Fullerene Dimer Dianion: $C_{120}O^{2-}$. *J. Chem. Phys.* **2008**, *128*, 114307.

(47) Neumark, D. N. Slow Electron Velocity-Map Imaging of Negative Ions: Applications to Spectroscopy and Dynamics. *J. Phys. Chem. A* **2008**, *112*, 13287−13301.

(48) Liu, H. T.; Ning, C. G.; Huang, D. L.; Wang, L. S. Vibrational Spectroscopy of the Dehydrogenated Uracil Radical via Autodetachment of Dipole-Bound Excited States of Cold Anions. *Angew. Chem., Int. Ed.* **2014**, *53*, 2464−2468.

(49) Huang, D. L.; Zhu, G. Z.; Wang, L. S. Observation of Dipole-Bound State and High-Resolution Photoelectron Imaging of Cold Acetate Anions. *J. Chem. Phys.* **2015**, *142*, 091103.

(50) Zhu, G. Z.; Liu, Y.; Wang, L. S. Observation of Excited Quadrupole-Bound States in Cold Anions. *Phys. Rev. Lett.* **2017**, *119*, 023002.

(51) Parker, S. F.; Bennington, S. M.; Taylor, J. W.; Herman, H.; Silverwood, I.; Albers, P.; Refson, K. Complete Assignment of the Vibrational Modes of C_{60} by Inelastic Neutron Scattering Spectroscopy and Periodic-DFT. *Phys. Chem. Chem. Phys.* **2011**, *13*, 7789−7804.

(52) Tagmatarchis, N.; Pichler, T.; Krause, M.; Kuzmany, H.; Shinohara, H. Infra-Red and Raman Spectroscopic Study on the Thermal Stability and High Temperature Transformation of Hydro-azafullerene $C_{59}HN$. *Carbon* **2006**, *44*, 1420−1424.

(53) Frisch, M. J.; Trucks, G. W.; Schlegel, H. B.; Scuseria, G. E.; Robb, M. A.; Cheeseman, J. R.; Scalmani, G.; Barone, V.; Mennucci, B.; Petersson, G. A.; et al. *Gaussian 09*, revision E.01., Gaussian, Inc.: Wallingford, CT, 2009.

(54) Wang, X. B.; Woo, H. K.; Huang, X.; Kappes, M. M.; Wang, L. S. Direct Experimental Probe of the On-Site Coulomb Repulsion in the Doubly Charged Fullerene Anion C_{70}^{2-}. *Phys. Rev. Lett.* **2006**, *96*, 143002.

(55) Wang, X. B.; Woo, H. K.; Yang, J.; Kappes, M. M.; Wang, L. S. Photoelectron Spectroscopy of Singly and Doubly Charged Higher Fullerenes at Low Temperatures: C_{76}^{-}, C_{78}^{-}, C_{84}^{-} and C_{76}^{2-}, C_{78}^{2-}, C_{84}^{2-}. *J. Phys. Chem. C* **2007**, *111*, 17684−17689.